Experimental Study of Axial Force Transfer through Pipes
-The Lateral Contact Force Effect-

INVESTIGATOR: Alexander Martinez
COMPLETION DATE: Fall, 1999.
SPONSORED BY: TUDRP

OBJECTIVES

- To evaluate experimentally the lateral contact force (LCF) between the pipe and the wellbore wall for straight and curved sections, and to compare with the current analytical models used to predict it.

PAST WORK

- Detailed literature review of papers related to buckling and post-buckling behavior of pipes constrained by a cylinder (inside the wellbore) and the lateral contact force between them.
- Design and assemble of the experimental horizontal facility.
- Set up and calibration of instrumentation required for the tests.

PRESENT WORK

- To measure the lateral contact for a straight horizontal section, using two systems.
  - Contact gage, the LCF was measured using the 0.750", 0.5" and 0.375 OD pipes.
  - Torque gage, the LCF was measured using the 0.750" and the 0.5 OD pipes.

FUTURE WORK

- To measure the lateral contact for a straight horizontal section, using the torque gage using the 0.750" and the 0.375 OD pipes.
- To measure the LCF for a straight pipe inside a curved section.
  - Design a device to measure the LCF in a curved section.
  - To measure the LCF using the appropriate OD size pipes.
- Comparison of the experimental results with the currently analytical models.

PRESENT STATUS

Task	***Description***	***Completion***
Literature Review	State-of-the-art	90%
Experiments	Assembling and Calibration of Experimental Facility	50%
	Contact Force Measurement Tests	45%
Computational Tool	Prediction of Drag Force	0%
Reports	ABM Reports and Final Report	50%

CONTENTS

INTRODUCTION……....1

1. LITERATURE REVIEW…….3

Mitchell, R. F., (1982), (1986), (1988) ……..…3

Sorenson, K. G., (1986) …… ……...3

Williams, T. H., Juvkam-Wold, H. C. (1995) ……3

Sadic, T. , Juvkam-Wold, H. C., (1995) ……..……4

2. STATEMENT OF THE PROBLEM ……...……..4

3. SUMMARY OF PAST WORK ……..…5

4. EXPERIMENTAL HORIZONTAL FACILITY …..……..…5

5. EXPERIMENTAL MEASUREMENTS OF THELATERAL CONATCT FORCE USING THE CONTACT GAGE ……..……8

5.1 Design of the contact gage ……...8

5.2 Experimental evaluation ……...11

6. EXPERIMENTAL MEASUREMENTS OF THELATERAL CONATCT FORCE USING THE TORQUE GAGE ……..……...19

6.1 Design of the contact gage …….19

6.2 Measurement of the friction coefficient ….……21

6.2.1 Static friction coefficient ….……...……..……22

6.2.1 Kinetic friction coefficient ….……...……..……23

6.3 Experimental results using the *torque gage* …….25

7. RESULT ANALYSIS ……..…….29

7.1 Friction coefficient ……..…..……29

7.2 Lateral contact force using the contact gage ….……...……..…….29

7.3 Lateral contact force using the torque gage …..……...…….…….30

8. FUTURE WORK ……....……...……..……30

REFERENCES ……....……...……..……...…32

INTRODUCTION

In directional and horizontal drilling, axial force transfer along the drill pipe is related to the drag force between the pipe and the hole. Several factors such as cuttings in the hole, geometry of the well, differential pressure, and frictional forces tend to increase the drag force. The frictional forces are a result of the pipe weight and the buckling compressive force on the pipe when the pipe is in a helix configuration.

A comprehensive literature survey was carried out on the buckling behavior of pipes constrained inside the well bore. The review reveled that additional frictional forces, for a buckling pipe, are caused by the generation of a lateral contact force between the pipe and the borehole. Considerable work has been done to estimate the lateral contact force by using analytical methods. As far as experimental evaluation is concerned, there is not much work reported in the literature. The results of the experimental work conducted by Sadic et. al. were found to contradict with the results of the analytical work done by Mitchell and others.

The main objective of this project is to evaluate experimentally the lateral contact force and to obtain our own results and conclusions.

This report describes the ways and means used to simulate the real field conditions in the design of the experimental facility, the different experimental approaches that were used to measure the lateral contact force, and the results obtained.

Two different systems were used to measure the lateral contact force. In section 5 information related to the design and experimental data obtained with the first approach (contact gage) is described. Due to some concerns about this approach, which are also addressed in this section, a second system was developed to measure the lateral contact force.

The design and experimental results of the second approach (torque gage) will be described in section 6. To use the second system, the friction factor between the pipe and the hole must be known. The procedure used to measure the friction factor is also described.

A preliminary comparison of the experimental results obtained by the two methods shows similar results. Considering that the two systems measuring the lateral contact force are totally different, it can be concluded that the values measured are accurate.

3. LITERATURE REVIEW

1.1 Mitchell, R. F., (1982), (1986), (1988).

R. Mitchell has been studying the buckling behavior of pipes since 1982. He developed the analytical expression to predict the lateral contact force for a helically buckled rod constrained in a cylinder.

$$W_n = \frac{rF_f^{\,2}}{4EI} \qquad (1)$$

where, Wn is the unitary contact force (lb/in), F_f is the axial force (lb), E the elastic modulus (psi), I the moment of inertia (in^4) of the pipe, and r the radial clearance (in).

Sorenson, K. (1984)

K. Sorenson also studied the helical behavior of pipes constrained inside the hole. Using an analytical approach, he developed a model to calculate the lateral contact force, his equation is similar to the one presented by Mitchell.

1.2 Williams, T. H., Juvkam-Wold, H. C. (1995)

In this paper are presented the results of an experimental study of the post-buckling frictional effects on a circular rod constrained inside a cylinder. The frictional forces

created by a helical pipe were studied and compared to the analytical equation developed by Mitchell. They concluded that Mitchell's lateral contact force equation seems to be accurate.

1.4 Sadic, T. , Juvkam-Wold, H. C., (1995)

The authors studied the post-buckling behavior of pipes and determined the lateral contact force. In their experimental approach, the lateral contact force was measured directly. They concluded that their data differs from the currently accepted Mitchell equation. They developed an equation to evaluate the lateral contact force. It is defined as:

$$W_n = \frac{rF^2}{2EI} \tag{2}$$

2. STATEMENT OF THE PROBLEM

The major objective of this research is to evaluate, experimentally, the lateral contact force (***LCF)*** between the pipe and the well bore wall, for lateral and helical post-buckling pipe configurations. The experiments will cover the simulation of horizontal and curved wellbore sections. Also, the experimental are compared with the currently available analytical models.

3. SUMMARY OF PAST WORK

At the beginning of this project, an extensive literature review was done. From this survey it was determined that there is a need to measure lateral contact force, LCF, in order to verify the analytical models currently available.

The experimental facility to simulate the horizontal wellbore was designed and assembled and the sizes of the pipes to be tested defined.

A device was designed to measure the lateral contact force, LCF. The system is composed of a pin that pushes the pipe in the radial direction, and a load cell that measure the pushing force. A more detailed description of this device will be presented in a later section.

4. EXPERIMENTAL HORIZONTAL FACILITY

The basic features of the horizontal facility used in this research are similar to the one used by Salies et. al. (1994) and Cunha et. al. (1996). Figure 1 is a schematic drawing of the facility. The features are:

- The total length of the horizontal facility is 86 ft,
- Inside diameter of the acrylic pipe, simulating the hole is 2 in
- Load cells are located at the top (to measure the applied load) and at the bottom (to measure the axial force transferred load).
- The application of the load to the pipe is controlled by the axial displacement of the top load cell, which is done by an electric motor with variable speed. Most of the tests were done at rate of displacement of 0.0005 in/sec.
- The displacement of the pipe, at the top, is measured with one LVDT, capacity: 6 in
- The facility has a data acquisition system having 16 channels. This records the signals from the load cells located at the top and bottom, the LVDT, and time

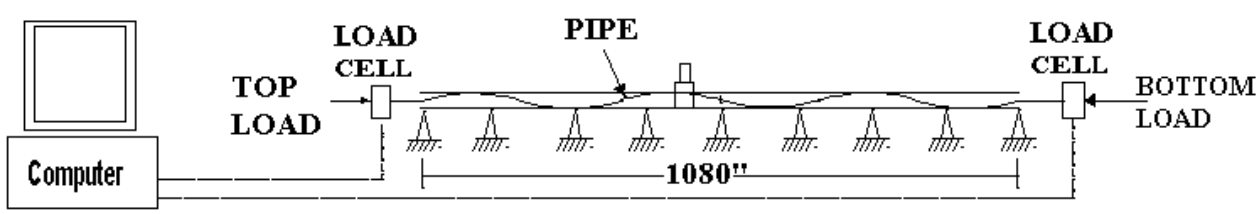

Figure 1. Horizontal facility setup.

The size of the pipes, to be used in the tests, was selected considering scale factor that represents the field pipe sizes. The scale factor is based on the relation *t/OD* (thickness/ outside diameter), and also on the relationship between the size of the hole and outside

diameter of the pipe. Table 1 presents the dimensions of the pipes that are being used in the tests. The pipes are made of stainless steel, seamless pipe and butt welded in 20 ft lengths.

	OD x t	Weight (lb/ft)	t/OD (%)	OD/ Hole (%)	Critical helical force	Maximum pitch length
Pipe 1	0.750 x 0.065	0.475	8.7	37.5	258 lb	25 ft
Pipe 2	0.5 x 0.049	0.236	9.8	25	533 lb	16.8 ft
Pipe 3	0.375 x 0.035	0.127	9.3	18.8	787 lb	14.6 ft

Table 1. Dimensions of the pipe that have been used in the experiments

The length of the pipes is also an important consideration, since, the buckling behavior of the pipes is highly affected by their length. The 86 ft length of the facility, which is the same length of the pipe, it is sufficient to produce multiple turn helix.

The other issue considered was the influence of end effects on the post-buckling behavior of pipes. According to the literature, the lateral contact force for a helical pipe is not constant for the first pitch length. The pipe must be able to develop a minimum of three pitches. This implies that the pitches close to the ends are not suitable for the tests, the ones located between these two pitches are being used for the tests.

The length of the pitch can be predicted by the following equation,

$$Picth = \pi \sqrt[4]{\frac{8EIr}{F}} \qquad (3)$$

where, EI is the stiffness of the pipe, r the radial clearance and the F critical helical force.

$$F_{hel} = 4\sqrt{\frac{2EIw}{r}} \qquad (4)$$

From Table 1, in terms of this requirement, the critical pipe would be the 3/4 OD pipe. For this pipe the pitch length is 25 ft, meaning that the pipe can develop a minimum of 3 pitches in its total length. During the tests, this pipe developed 5 pitches.

5. EXPERIMENTAL MEASUREMENTS OF THE LATERAL CONTACT FORCE USING THE CONTACT GAGE

5.1 Design of the contact gage.

A special device was designed to measure the lateral contact force. Figure 2 shows this measuring device, that is referenced as the ***Contact Gage***. The principle of the contact gage is the generation of a force in the opposite direction of the lateral contact force of the pipe. The *contact gage* is composed of the following elements:

- A pin that moves radially pushing the pipe. The pin is in direct contact with the pipe.
- A load cell that measures the pushing force of the pin against the pipe.
- A screw system that control the displacement of the pin
- An indicator that measures the displacement of the pin.

The contact gage is located on a window, as observed in Figure 2. The wellbore is represented by short sections of acrylic pipe (3 ft each). Between each acrylic section there is a gap (1 in), which is “the window”. The *contact gage* can be placed on any one of these windows located along the pipe. Other important feature of the gage is its ability to measure the contact force for any position of pipe, with respect to the hole.

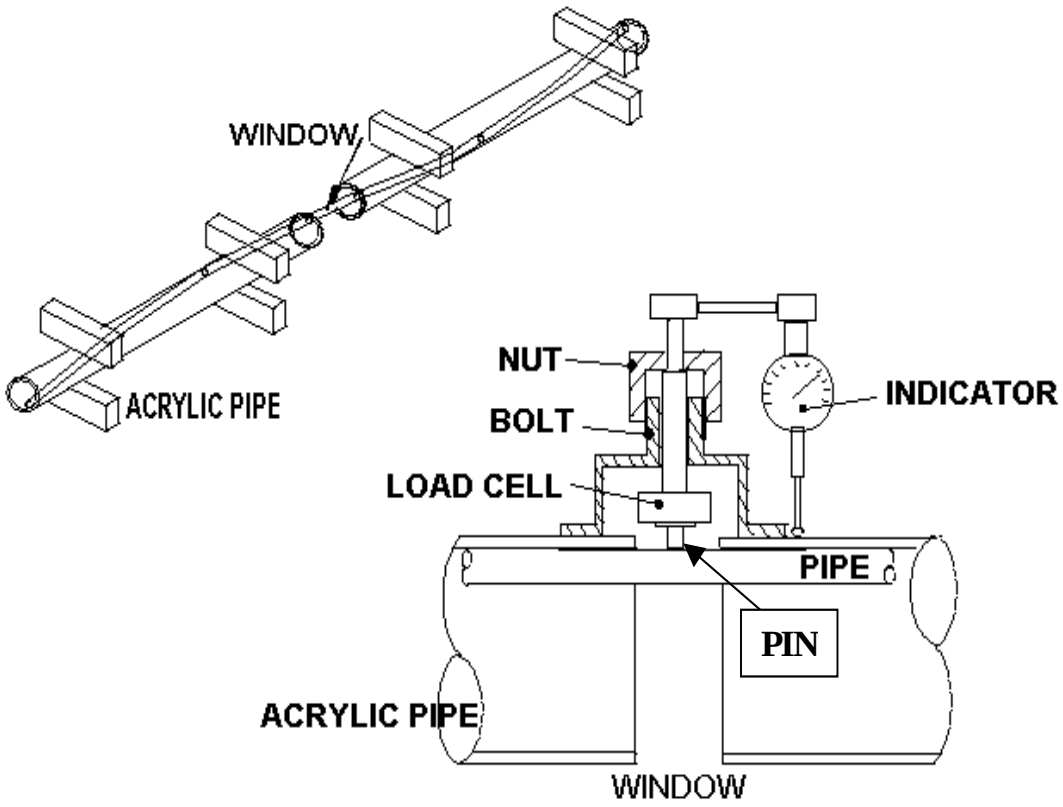

Figure 2. Illustration of the *contact gage* to measure the lateral contact force.

Figure 3 is a typical plot that shows the force measured by the load cell of *the contact gage*, versus the displacement of the pin. As it can be seen, initially, for very small radial

displacement of the pin (values lower than 0.006 in), the force increases rapidly. Following this, the force continues to increase but at a lesser rate. Each curve represents a different level of compressive force applied to the pipe.

Initially, it was considered that the load where the curve changes slope was related to linear lateral contact force for the length of pipe. Then dividing this force by the length of the window will give the unitary lateral contact force.

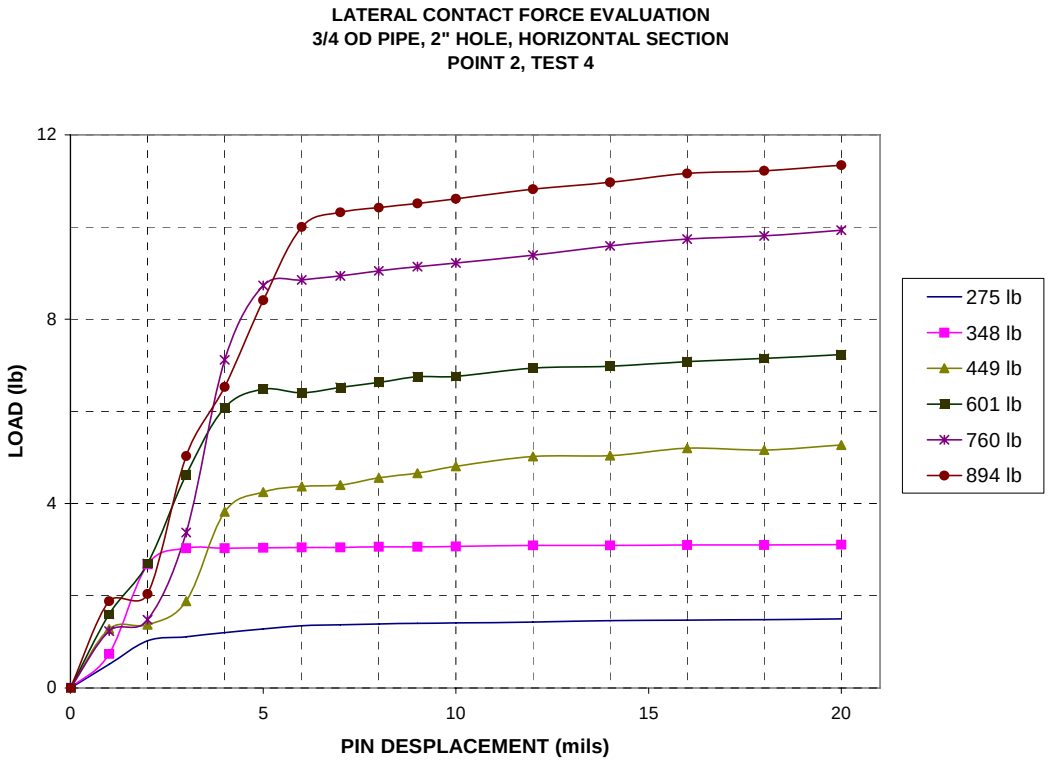

Figure 3. Typical plot of radial displacement versus pin force.

5.2 Experimental evaluation.

The tests using the *contact gage* were done as follows:

- Applying load at the top, the pipe is buckled into a helical shape. Then the applied displacement is kept constant.
- The lateral contact force is measured at four different locations along the pipe.
- The compressive force is increased and the displacement is locked.
- The lateral contact force is measured again at the same locations.
- The top load is increased in intervals and the LCF is measured for each increment.
- This process is done until the pipe reaches a pre-established limit for every one of the pipes, which prevents plastic deformation.

Following this procedure, tests were conducted on the 0.750" OD, 0.50" OD and 0.375" OD pipes, Figure 4, 5, and 6 present the experimental results for each of these pipes, the abscissa axis is the applied top compressive force, and the ordinate is the value measured by the load cell of the *contact gage*. Also, the curves of the predicted values using the analytical equations (Eq. 1 and 2) are included.

There is a common characteristic among these figures. The experimental results are much higher than the values predicted analytically. In order to validate the experimental results, some additional tests were conducted.

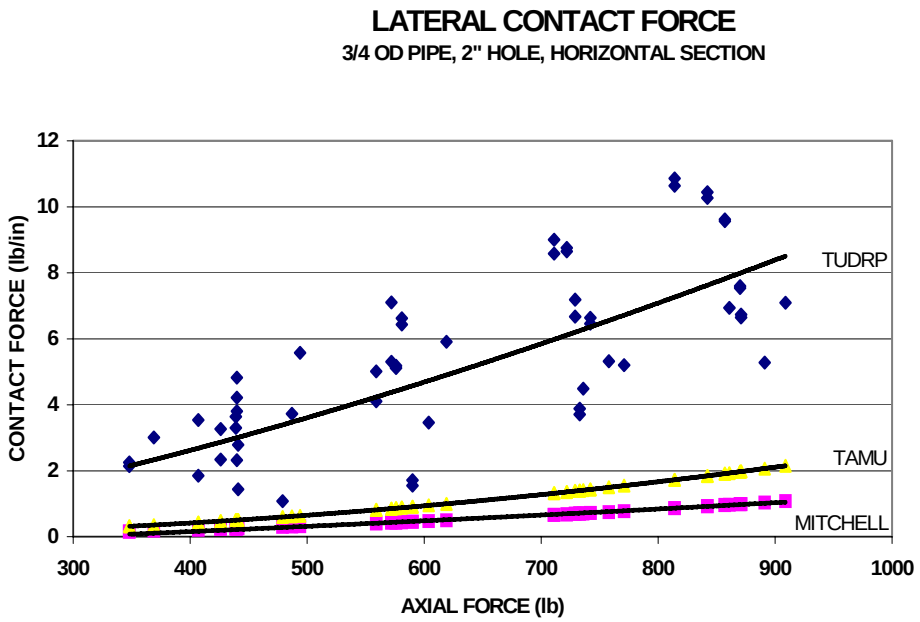

Figure 4. Lateral contact force using the *contact gage*, 0.750"" OD pipe in 2" ID hole.

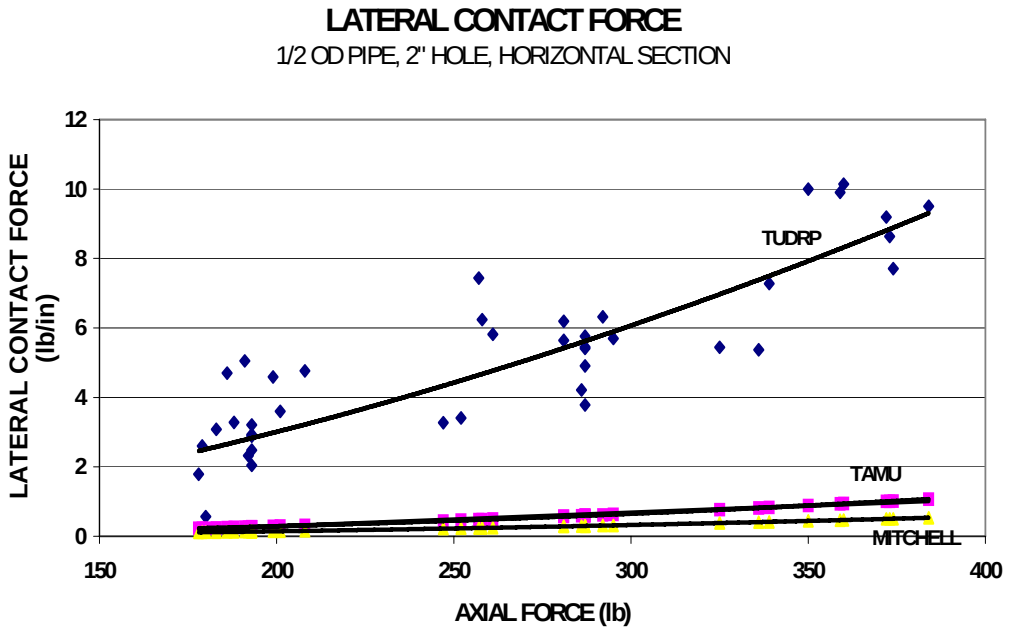

Figure 5. Lateral contact force using the *contact gage*, 0.50" OD pipe in 2" ID hole.

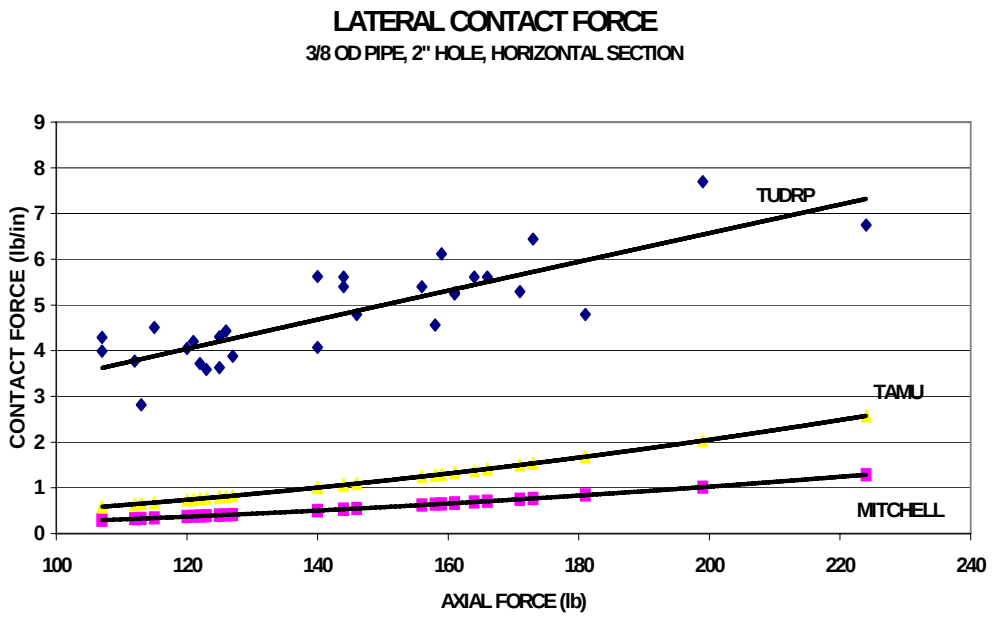

Figure 6. Lateral contact force using the *contact gage*, 3/8 " OD pipe, 2 in ID hole.

The main objective of these tests was to identify the influence of the window and pin size on the force measured by the contact gage. In these tests the size of the window was changed, from 0.5 in to 2 in, and the diameter of the pin from 0.25" to 1". The experimental results, incorporating these changes, varied little from earlier tests. It was concluded that the contact force measured by the *contact gage* was not affected by these variables.

A close visual observation was performed to identify the behavior of the pipe. It was found that as the pipe moves radially, due to the pin that is pushing it, the pipe separates longitudinally from the well bore wall. This length of separation is on the order of inches,

while the radial displacement is in the order of in/1000 (mils). This implies that the high values of force measured by the gage were related to the total separation of the pipe.

To calculate the unitary contact force, the force measured by the gage must be divided by the separation length. To do this calculation the separation length must be known. The length is defined by the distance between the two points where the pipe lost contact to the wall. To visually accurately measure where these two points or tangential points are located is almost impossible. To overcome this problem an analytical method of analysis was needed.

A simple analytical model was developed, to calculate the length of separation. The model assumes a straight pipe, with a constant lineally distributed load, as depicted in Figure 7. The resulting expressions are as follows:

$$N_u = \sqrt[3]{\frac{F^4}{384\ EI\ v}} \qquad (5)$$

$$L_s = \sqrt[3]{\frac{384\ EI\ v}{F}} \qquad (6)$$

Where: N_u: unitary lateral contact force (lb/in)

L_s: length of separation (in)

F: pushing force (lbf), force measured by the *contact gage* .

v: radial displacement or deflection (in), or value measured by the indicator of the contact gage

E: elastic modulus (psi)

I: moment of inertia (in^4)

L_s: Longitudinal separation of the pipe without touching the wall. (in)

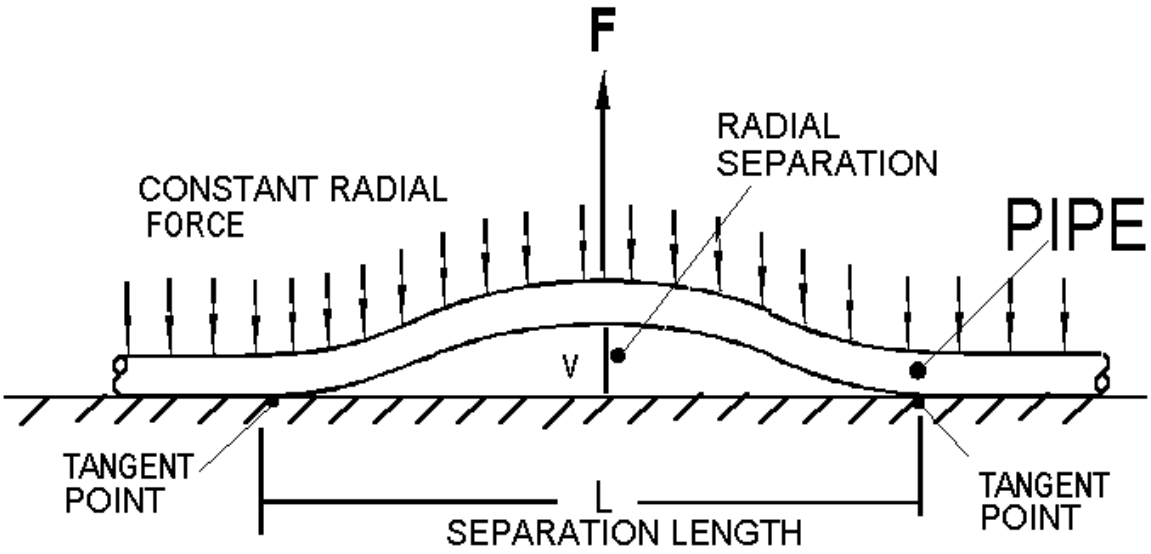

Figure 7. Simulation of longitudinal separation of the pipe from the wellbore wall. In this drawing the radial separation is exaggerated.

Figure 8 shows the value of radial force, *F*, versus radial displacement, *v*, using the proposed analytical model (Eq. 5). Each curve in Figure 8 represents a different contact force. As it can be seen, the pattern of the curves is similar to the pattern of the curves of Figure 3. Initially, for very small values of radial displacement, the contact force increases sharply, then continues to increase at a lower rate.

Figure 9 represent the length of separation (longitudinal length) versus the radial displacement of the pipe, using Eq. 8. Each curve in Figure 9 represents a different contact force. These curves show that for very small radial displacement of the pipe, the longitudinal separation is in the order of inches. This analytical approach explains the high values measured using the *contact gage*.

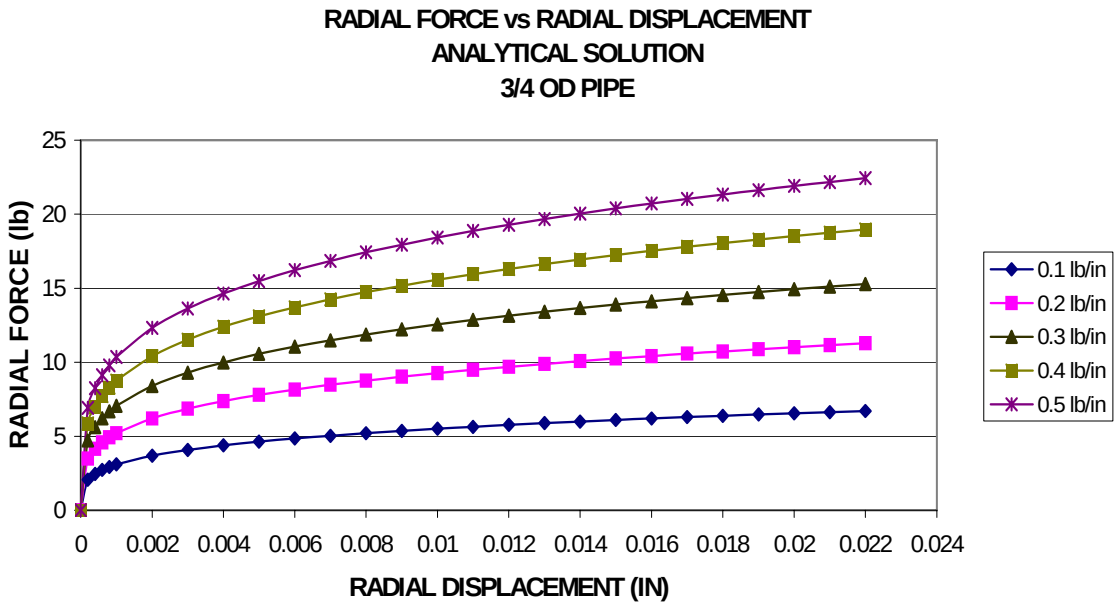

Figure 8. The figure depicts the pushing force, F, versus radial displacement of the pipe, v, using Eq. 7. Each curved is specified for a different value of lateral contact force.

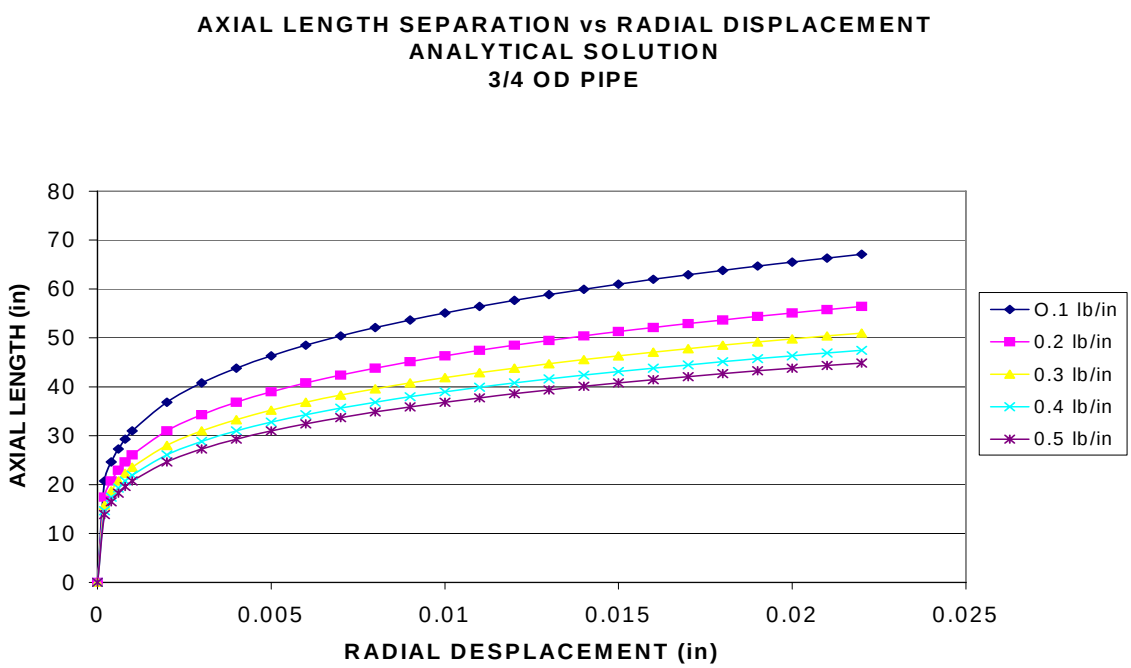

Figure 9. Longitudinal separation L, versus radial displacement of the pipe, v, using Eq. 8. Each curve is for a different value of lateral contact force.

Assuming that the analytical model (Eqs. 5, Figure 8) simulates the behavior of the data measured by the contact gage, (Figure 3), both systems were combined. Using the experimental data of the radial displacement of the pin and the force relative to this displacement, and then applying Equation 7, the unitary lateral contact force can be determined.

Using this combined approach, all the experimental data was corrected in order to calculate the unitary lateral contact force. Figures 10, 11 and 12 show the results for ¾" OD, ½" OD and 3/8" OD pipe respectively. The abscissa represents the axial force of the pipe, and the ordinate axis is the unitary lateral contact force.

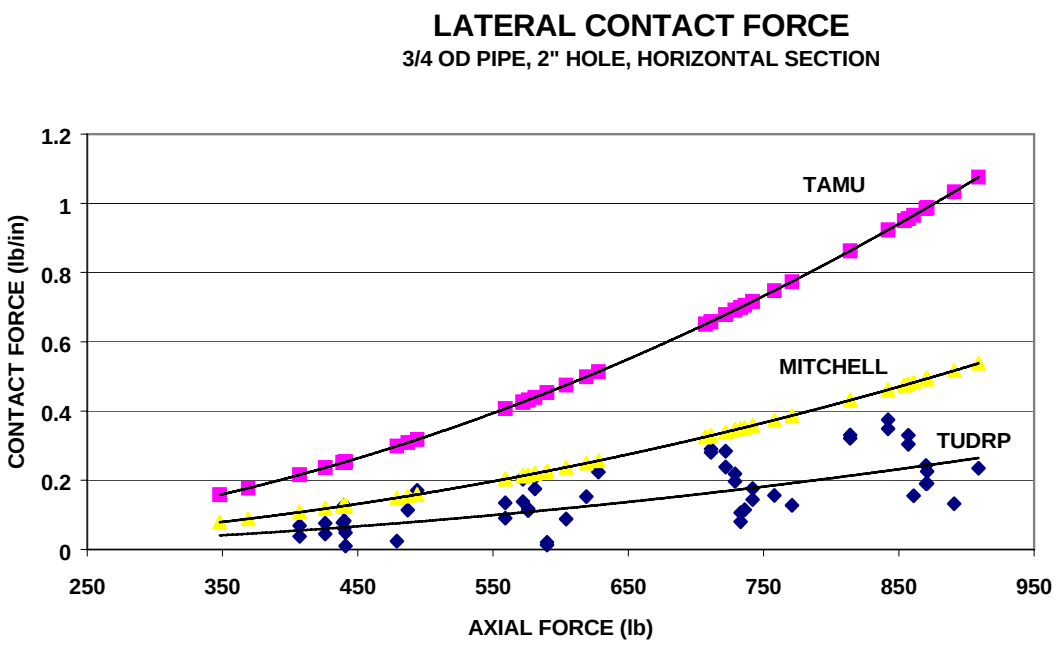

Figure 10. Unitary lateral Contact Force versus axial force of the pipe, using the combined approach. 3/4" OD pipe.

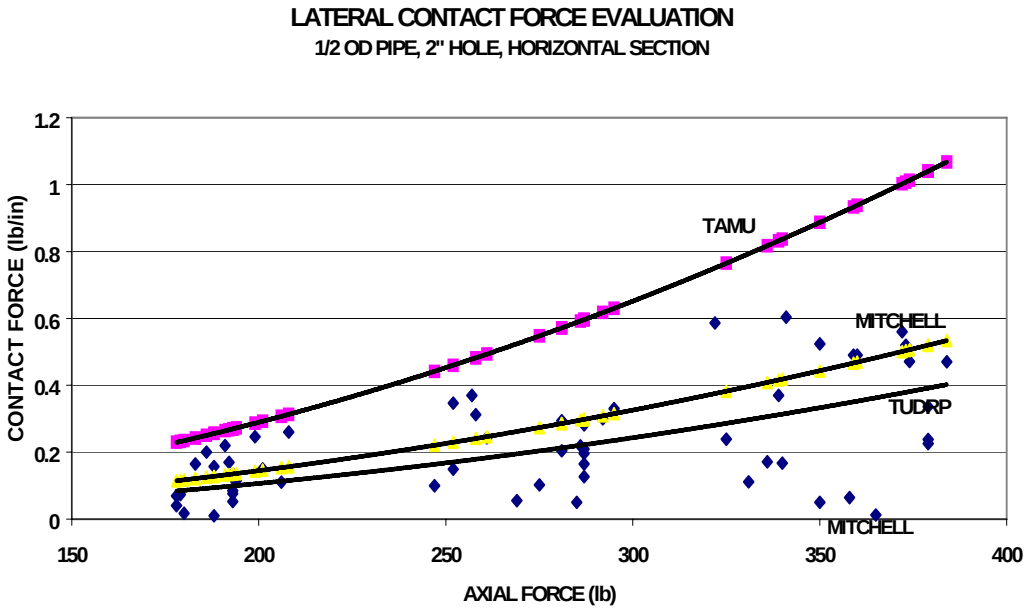

Figure 11. Unitary lateral contact force versus axial force of the pipe, using the combined approach. 1/2" OD pipe.

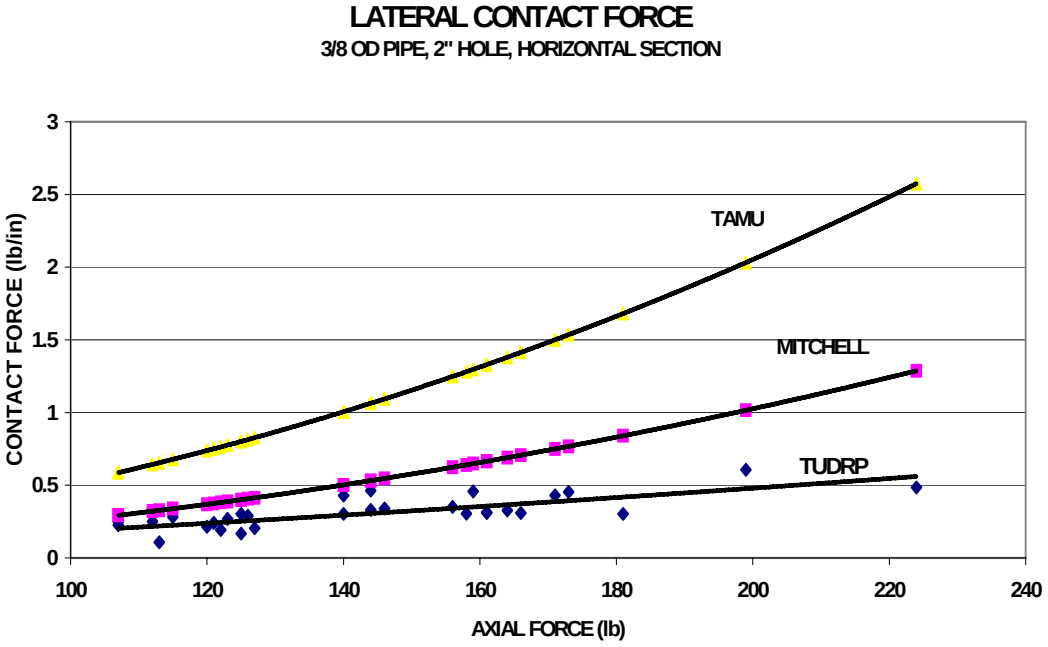

Figure 12. Unitary lateral contact force versus axial of the pipe, using the combined approach. 3/8" OD pipe.

6. EXPERIMENTAL MEASUREMENT OF THE LATERAL CONTACT FORCE USING THE TORQUE GAGE

Due to the fact that the *contact gage* system measures the unitary contact force in combination with an analytical solution, the main objective of this research, experimental approach, is not fully fulfilled. An attempt was made to accomplish this objective by designing a new experimental system .

A simple experimental system was develop based on torsion. The system measures the LCF in an indirect way. The load gage measures the force necessary to rotate the pipe around its longitudinal axis, then using a force balance equation, the unitary lateral contact force is calculated. This system is called the *torque gage*.

6.1 Design of the *torque gage*.

The *torque gage* is shown in Figure 13. A section of the hole, acrylic pipe, is rotated. The load cell measures the force necessary to keep the acrylic pipe in rotation at constant rate. An electrical motor controls the velocity of displacement of the load cell, making the acrylic pipe rotate at very low angular velocity (0.2° per second). The *torque gage* was

installed at three different locations along the pipe at 24 ft, 40 ft and 64 ft (from the top end).

From a force balance equation, the unitary lateral contact force is calculated using the following equation.

$$N_u = \mu \frac{F}{L} \frac{R_1}{R_2} \tag{7}$$

where:
- N_u : unitary lateral contact force,
- μ: friction coefficient,
- F: axial force at the point,
- L: section of acrylic pipe that rotates,
- R1: radius of the internal acrylic pipe,
- R2: radius of the pulley.

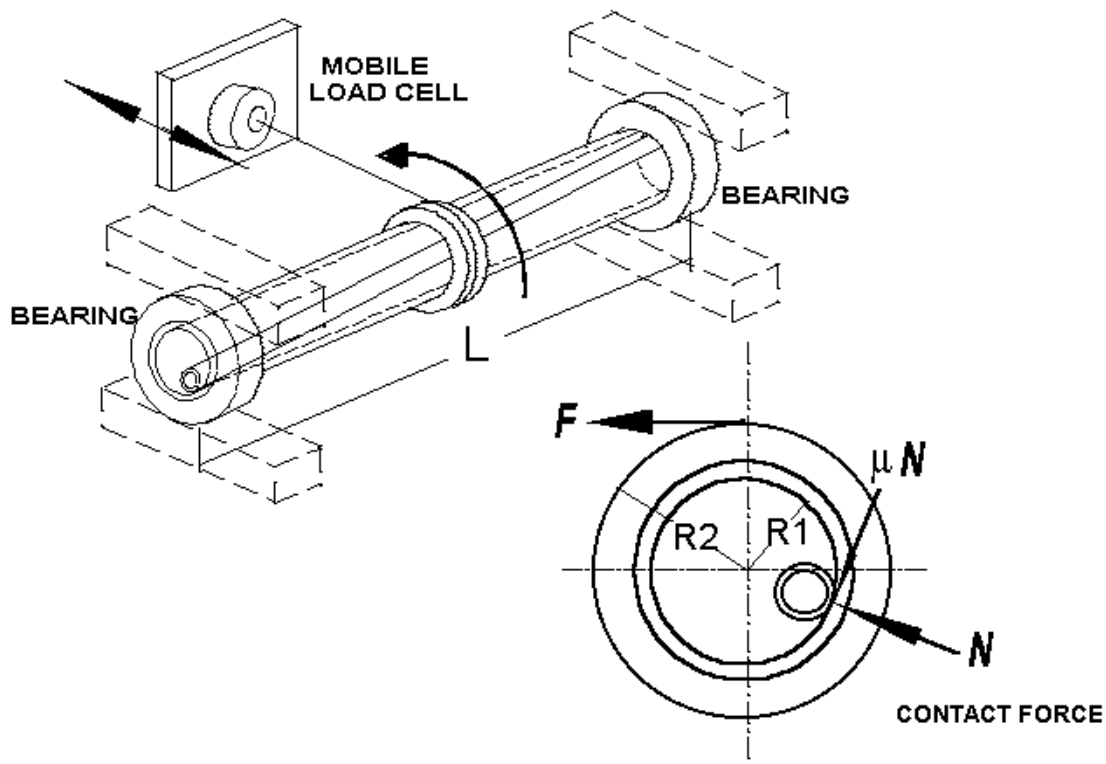

Figure 13. LCF measure system using the *torque gage*.

6.2 Measurement of friction coefficient.

To calculate the LCF, using the *torque gage*, it is necessary to know the friction coefficient between the pipe and the simulated hole (acrylic pipe). According to the simple physical phenomena related to friction between two bodies, the friction could be static or kinetic. The static friction is evaluated when there is no relative movement between the bodies, and the kinetic friction applies when there is a relative movement between the bodies. Figure 14 depicts the way both kinds of friction factors were measured.

To measure the friction coefficient the entire pipe, inside the hole, was used. The top load cell was displaced at a very low velocity (0.0005 in/s). It was used as the pulled element and also as the measured device.

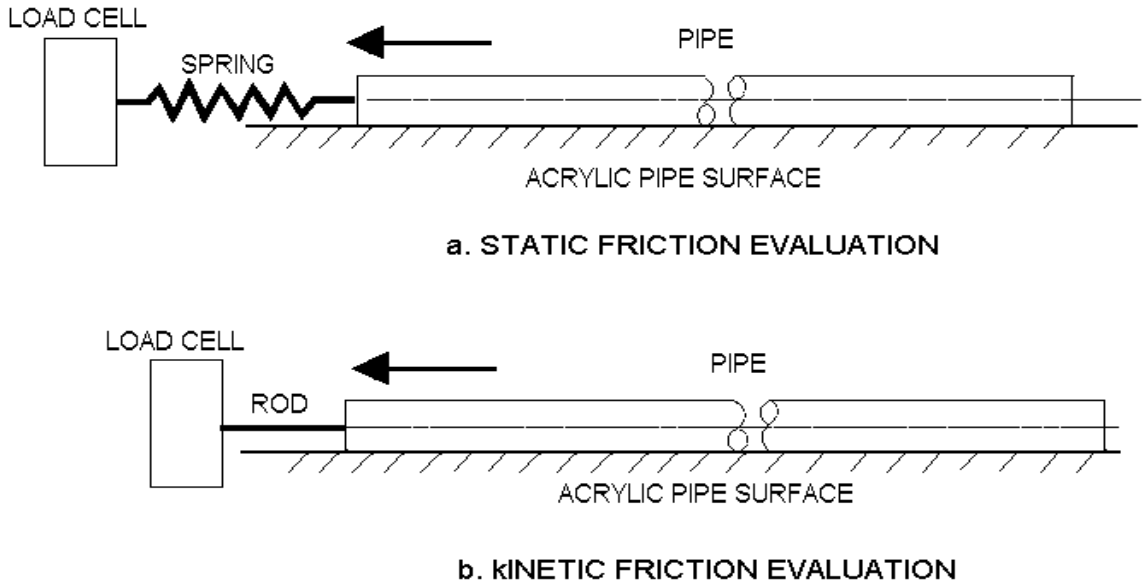

Figure 14. The figure depicts how the static and kinetic friction coefficients are measured.

6.2.1 Static friction coefficient.

Figure 14a shows how the static friction factor was measured. In order to keep the pipe static, while the pulling force was increasing, a balance spring was used in between the pipe and the load cell.

Figure 15 shows the results of the test done using the 1/2" OD pipe. The plot shows how the force or load measured by the gage changes during the test. Initially, the load increases from zero to a maximum value of 8.7 lb. At this value, the force is capable of moving the pipe. As the pipe moves, the force applied by the load cell is decreased due to the presence of the balance spring. Then the pipe stops moving, at 6 lb. If the load cell keeps moving the process is repeated again.

The static friction coefficient is the relation between the maximum load recorded by the load cell and the weight of the pipe. For the 0.5 OD pipe we get:

$$\mu_s = \frac{F_{max,\,static}}{W_{pipe}} = \frac{8.5lb}{0.236lb/\ ft\ x\ 86\ ft} = 0.41$$

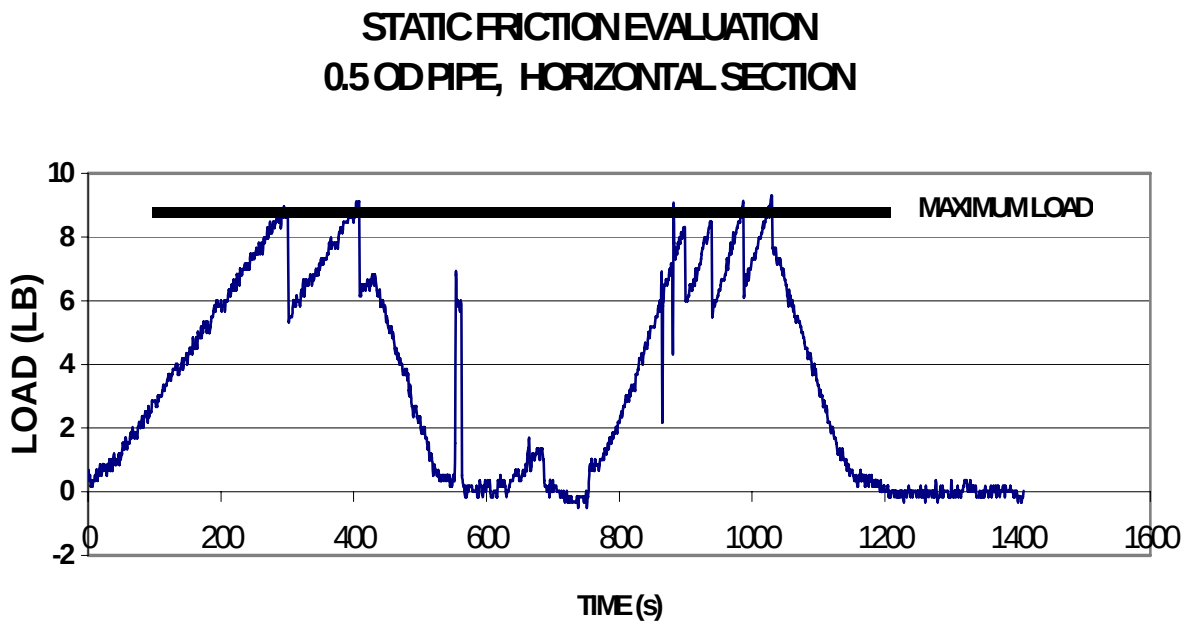

Figure 15. Static friction coefficient evaluation.

6.2.2 Kinetic friction coefficient.

To calculate kinetic friction coefficient, the pipe is kept moving inside the wellbore. For this test, taking advantages of the experimental facility, the load cell is in direct contact with the pipe pushing it. The pipe, when straight, is free to move inside the hole, while the load cell measures the pushing force moving the pipe. The pipe moves at the same velocity as the load cell does.

Figure 16 shows the experimental results of the kinetic friction coefficient evaluation. Time on the abscissa relates the application load rate, and on the ordinate axis is the load measured by the top load cell.

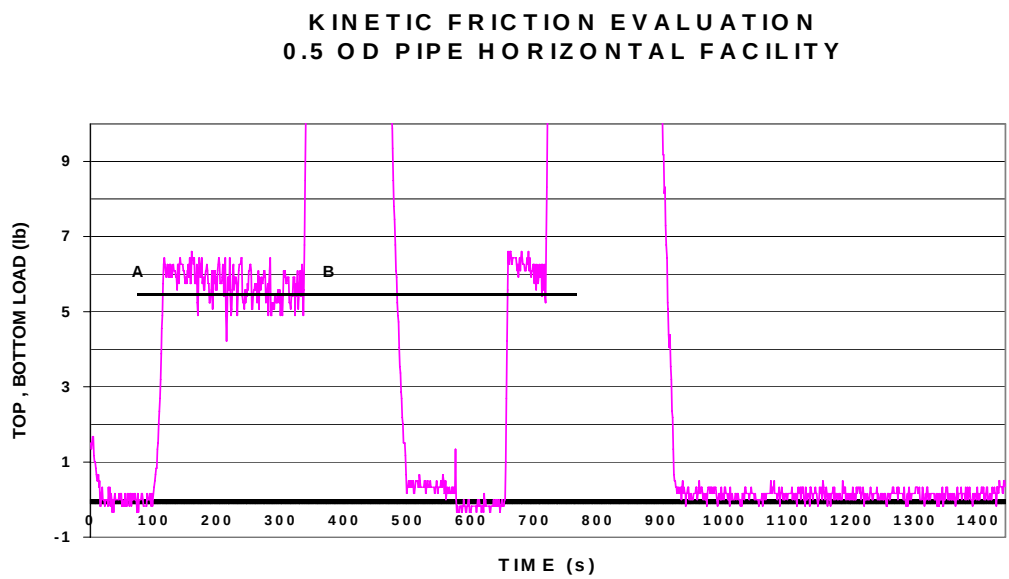

Figure 16. Kinetic friction coefficient evaluation.

Initially, when the load cell moves without touching the pipe, the load is zero. At point A the load cell starts contacting the pipe, then the pipe starts moving with the load cell. The load measured by the cell remains constant (5.7 lb). This load remains constant while the pipe moves freely inside the hole, from A to B. At point B, the pipe starts contacting the bottom load cell, stopping its movement and converting the pushing force into a compressive force.

The friction factor is the relation between the maximum pushing force measured by the load cell and the weight of the pipe. For a 0.5" OD pipe, it gives us,

$$\mu_K = \frac{F_{max,\,kinetic}}{W_{pipe}} = \frac{5.7\ lb}{0.236 lb/\ ft\ x\ 86\ ft} = 0.28$$

The kinetic friction factor was also evaluated using the 0.750" OD pipe, the results were very close to ***0.28.***

6.3 Experimental results using the *torque gage*.

These tests are done in parallel, meaning that as the axial load of the pipe is increasing, at the same time the torque gage measures the force necessary to rotate the acrylic pipe. During the execution of the test, there is relative movement between the pipe and the acrylic pipe. Due to this relative movement between the pipes, the friction coefficient that must be used in the calculations of the LCF is the kinetic friction factor.

Figure 17 shows the experimental values of lateral contact force for the 0.750” OD pipe. This plot presents the experimental results and the predicted values using Eqs. 1 and 2. The abscissa corresponds to the axial force transmitted by the pipe, at the segment where the contact force was measured, and the ordinate is the measured value of the lateral contact force. The Figure also shows different curves for different friction coefficients used in Eq. 5. The friction coefficient is a critical parameter in the calculation of lateral contact force using the present method.

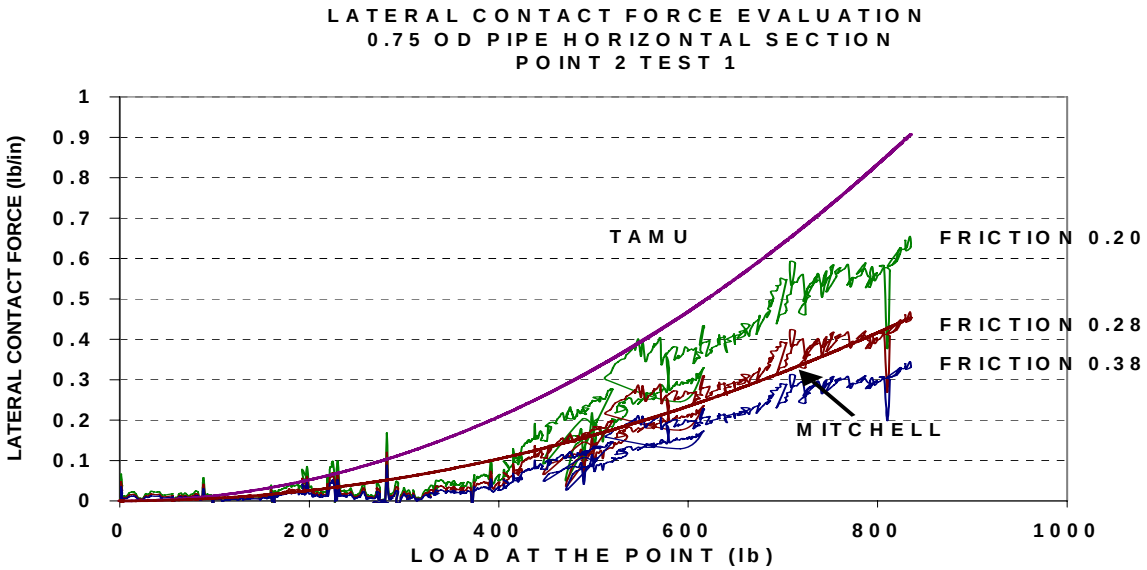

Figure 17. Lateral contact force measured with the *Torque gage* and using different values of friction coefficient.

To compare the experimental data with the analytical models, (Eq, 1 and Eq 2), the axial force must be higher than the critical helical force. This means that the pipe must be in a helical shape. In Figure 17, the comparison between the experimental data and the predicted values is valid for axial forces higher than 500 lb.

Figure 18 is another test done using the ¾” OD pipe. The friction coefficient applied was 0.28. The experimental values are smaller than predicted ones. The trend of the curve of the experimental data is similar to the predicted ones.

Figures 19 and 20 are the experimental results using the 0.5” OD pipe. Figure 19 shows the results when the torque gage was installed at point 2 (40 ft from the top). The experimental data shows good repeatability, and the values are always smaller than the predicted ones. The trend of these curves is similar to the trend of the curves of the predicted values.

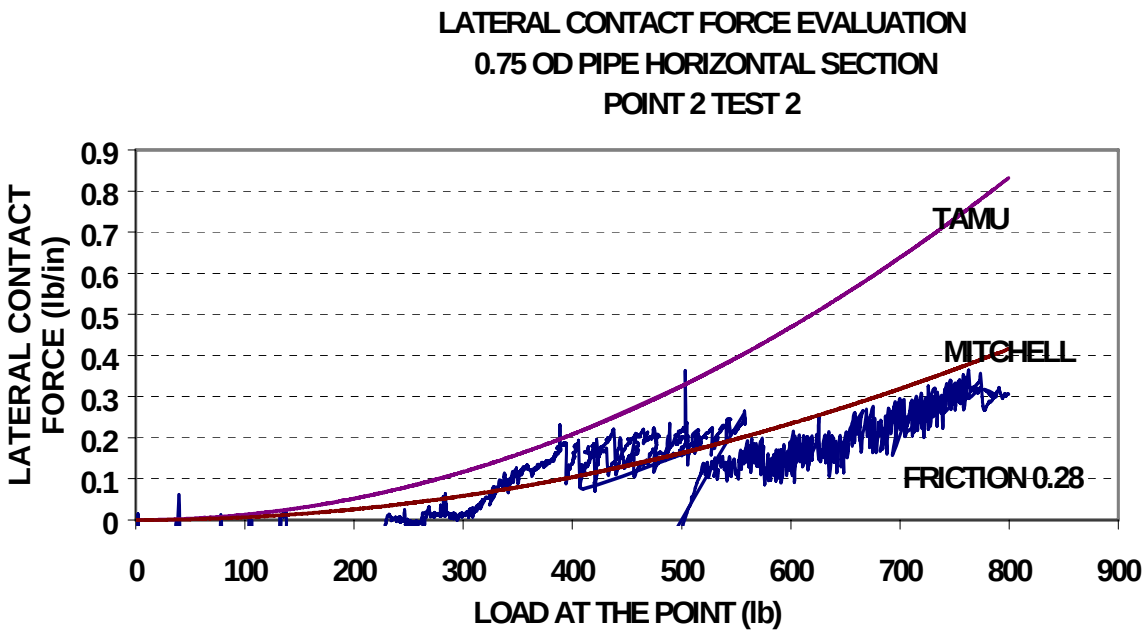

Figure 18. Experimental results on the evaluation of the lateral contact force using the torque gage, ¾ OD pipe, 0.28 friction coefficient.

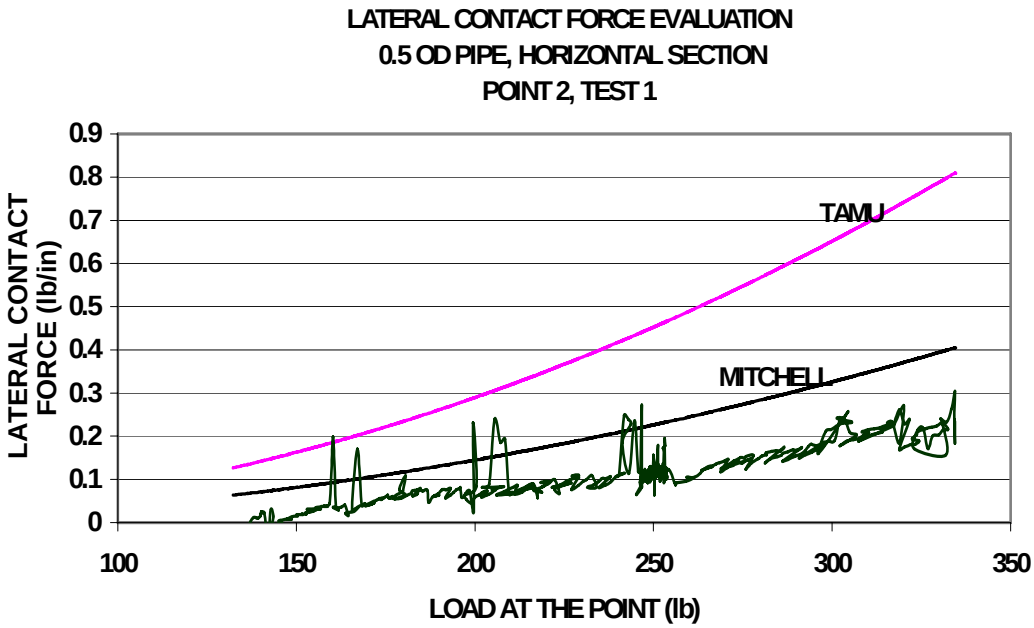

Figure 19. Lateral contact force using the Torque gage method, point 2 is located at 40ft from the top end.

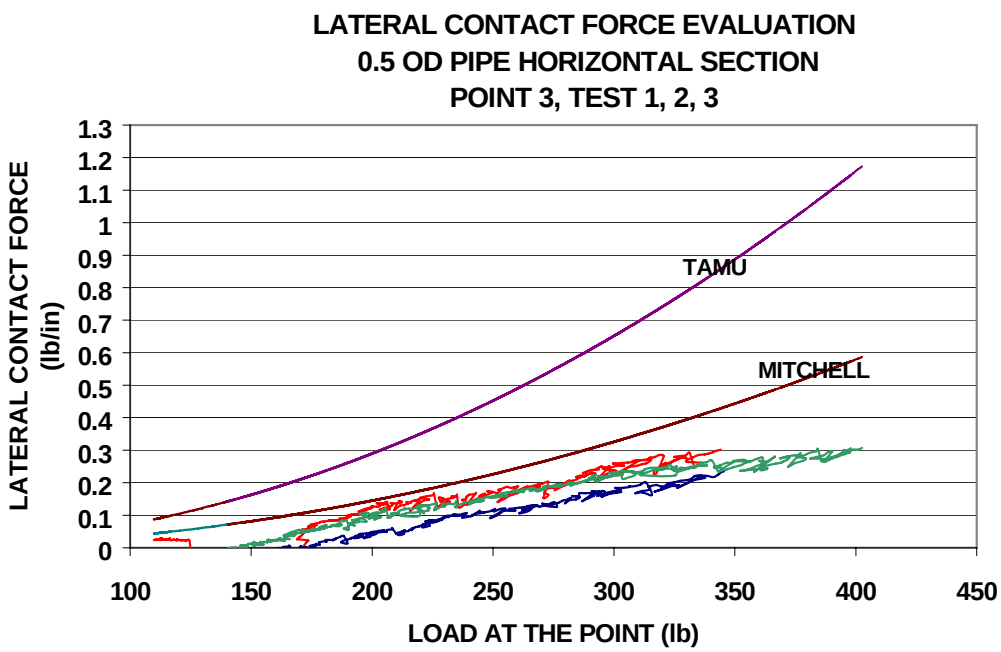

Figure 20. Lateral contact force using the Torque gage method. Three different tests are plotting. 0.5 OD pipe, Point 3 located 65 ft from top end.

7. RESULT ANALYSIS

7.1 Friction Factor

The experimental value of the static friction coefficient between the stainless steel pipe and the acrylic is **0.41**, while the kinetic friction coefficient is only **0.28**. According to literature, the static friction is always higher than the kinetic one. Several tests were done using 0.5" OD and 0.750" OD pipes, the results are all very close to these values.

There is a relative motion between the pipes (stainless steel and acrylic) when the *torque gage* is used to measure the LCF. This implies that the kinetic friction must be used in these calculations of the LCF.

7.2 Lateral Contact Force, using the *contact gage*.

In Figures 11, 12 and 13, comparison of the experimental data to the analytically predicted values, shows that the experimental results are lower that the predicted ones. In Figure 12, there is a scattering of the data, but the average of all the data together is less than also smaller than the predicted values.

7.3 Lateral Contact Force, using the *torque gage*.

Figure 16, 17, 18 and 19 show the experimental values measured using the *torque gage*. The experimental data in all the cases were smaller than the predicted values. This behavior is the same as the one showed by the experimental data measured with the *contact gage*.

The experimental data of Figure 17 compared with the data of Figure 16, using the kinetic friction factor of 0.28, shows a slight difference. At present, further tests on 0.750” OD pipe are in process. Also, the tests for 0.375” OD must be carried out. Once these tests are completed, a concise evaluation can be made.

8. FUTURE WORK

8.1 Horizontal section.

- Additional tests to be done with the 0.750” OD pipe, using the *torque gage*.
- The *torque gage* method will be used in the evaluation of LCF using the 0.375” OD pipe.
- Integral analysis of all the data.

8.2 Curved section

- Design and assembly of the experimental facility.
- A new system to be designed to measure the lateral contact force.
- Execute the tests, using predetermined pipe sizes.
- Integral analysis of all the data.
- Comparison of the data, with the current analytical models

REFERENCES

Lubinski, A. " Developments in Petroleum Engineering- Collected works of Arthur Lubinski" Edited by Stefan Miska, Gulf Publishing Company, 1987.

Mitchell, R.F.; " Buckling Behavior of Well Tubing: The Packer Effect", SPE 9264, Society Of Petroleum Journal, 1982.

Mitchell, R.F.; " Frictional Forces in Helical Buckling of Tubing", SPE 13064, presented at the 59th Annual Technical Conference and Exhibition, Houston, USA, September 1984.

Mitchell, R.F.; " Simple Frictional Forces in Helical Buckling of Tubing", SPE 13064, SPE Drilling Engineering, December 1986.

Mitchell, R.F.; " Numerical Analysis of Helical Buckling of Tubing", SPE 14981, presented at the Deep Drilling and Production Symposium Of SPE of AIME, Amarillo, Texas, April 1986.

Mitchell, R.F.; " New Concepts of Helical Buckling", SPE 15470, SPE Drilling Engineering, September 1988.

Mitchell, R.F.; "Buckling Analysis in Deviated Wells: A Practical Method", SPE 36761, presented at the SPE Annual Technical Conference and Exhibition, Denver, USA, October 1996.

Sorenson, K.G., "Post buckling behavior of a circular rod constrained within a circular cylinder", Ph. D. Dissertation, Rice University, Houston, USA, 1984.

Williams, T. H., Juvkam-Wold, H.C.; “An Experimental Study of the Post Buckling Frictional Effects of Drillpipe in a Horizontal well:”, CADE/CAODC Spring Drilling Conference, Paper 93-506, Calgary, Canada, April 1995.

Sadiq, T., Juvkam-Wold, H.C.; “ Lateral Contact Force in horizontal well: An Experimental Study”, CADE/CAODC Spring Drilling Conference, Paper 93-503, Calgary, Canada, April 1995.

Salies, J.B.; “ Experimental Study and Mathematical Modeling of Helical Buckling of Tubulars in Inclined Wellbores”, Ph.D. Dissertation, Tulsa University Drilling Research Projects, 1994.

Cunha, J.C.; “ Buckling Behavior of Tubulars in Oil and Gas Wells, A Theoretical and Experimental with Emphasis on the Torque Effect”, PhD Dissertation, Tulsa University Drilling Research Projects, 1995.

Wu, J. Juvkam-Wold, H.C.; " Coiled Tubing Buckling Implication in Drilling and Completing Horizontal Wells", SPE Drilling & Completion, March 1995.

Martinez, A. " Experimental Study of Axial Force Transfer Through Pipes- The Lateral Contact Force Effect-" Advisory Board Meeting Report, November 1999.